Centre–surround inhibition among olfactory bulb glomeruli

J. L. Aungst[1]*, **P. M. Heyward**[1]*†, **A. C. Puche**[1]*, **S. V. Karnup**[1], **A. Hayar**[1], **G. Szabo**[2] & **M. T. Shipley**[1]

[1]*Department of Anatomy and Neurobiology, Program in Neuroscience, The University of Maryland School of Medicine, Room 222, 685 West Baltimore Street, Baltimore, Maryland 21201, USA*
[2]*Department of Gene Technology and Developmental Neurobiology, Institute of Experimental Medicine, Budapest, Hungary*

* These authors contributed equally to this work
† Present address: Department of Physiology, Otago School of Medical Sciences, University of Otago, Dunedin, 9001, New Zealand

....

Centre–surround inhibition—the suppression of activity of neighbouring cells by a central group of neurons—is a fundamental mechanism that increases contrast in patterned sensory processing. The initial stage of neural processing in olfaction occurs in olfactory bulb glomeruli, but evidence for functional interactions between glomeruli is fragmentary. Here we show that the so-called 'short axon' cells, contrary to their name, send interglomerular axons over long distances to form excitatory synapses with inhibitory periglomerular neurons up to 20–30 glomeruli away. Interglomerular excitation of these periglomerular cells potently inhibits mitral cells and forms an on-centre, off-surround circuit. This interglomerular centre–surround inhibitory network, along with the well-established mitral–granule–mitral inhibitory circuit, forms a serial, two-stage inhibitory circuit that could enhance spatiotemporal responses to odours.

Odour perception begins with the binding of odorant molecules to specific receptors expressed by olfactory receptor neurons (ORN). Each ORN expresses a single odorant receptor from a repertoire of ~1,000 genes[1]. ORN axons project to the main olfactory bulb (MOB), where they synapse onto the dendrites of second-order neurons in spheroidal structures—glomeruli. Individual odorant receptors are broadly tuned: a given receptor is activated by many odours and, conversely, an odour activates many different receptors. As each glomerulus is innervated by ORNs expressing the same odorant receptor[1–5], different odours produce unique patterns of multiglomerular activation[6–14]. Therefore, odour perception requires the neural computation of patterns of glomerular activity.

Current hypotheses of MOB function hold that lateral interactions between mitral/tufted output cells, mediated by inhibitory granule cells, are fundamental to the processing of spatiotemporal patterns of glomerular activity[15,16]. Strongly activated mitral/tufted cells inhibit weakly activated ones through dendrodendritic synapses with granule cells. This is thought to enhance discrimination at the level of MOB output. Lateral interactions may also occur at the level of olfactory nerve input through connections between glomeruli[17]. Although interglomerular connections have been suggested by classical Golgi and electron microscopy (EM) studies[18,19], the magnitude and spatial extent of these connections are unknown, and physiological evidence for interglomerular interactions is lacking. The goal of the present study, therefore, was to determine the anatomical basis for and functional significance of interglomerular connections.

Extensive interglomerular connections

To investigate the anatomical basis of interglomerular projections, small tracer injections were made into the glomerular layer of the intact mouse MOB to label juxtaglomerular (JG) cells that give rise to interglomerular connections (Fig. 1 and Supplementary Fig. 1). A single subglomerular iontophoretic injection of DiI (5–10 μm diameter) was made into each MOB (Fig. 1a). Analysis of labelled JG cell distributions (48.5 ± 8 cells per MOB, $n = 6$; Fig. 1b–e) showed that 50% of labelled cells were located at distances greater than 350 μm (~5–7 glomeruli) from the injection site, and 10% were at distances greater than 850 μm (~15–18 glomeruli). As all injection sites were smaller than the diameter of a single glomerulus

(50–100 μm), these results underestimate the number of cells projecting to a single glomerulus, but do show that interglomerular connections extend over much greater distances than was previously thought. Labelled JG cells were distributed radially with no significant rostrocaudal or dorsoventral anisotropy (Fig. 1c, d). Identical tracing experiments in rats showed that interglomerular projections were organized as in mice (75.3 ± 8.8 cells per MOB, $n = 3$ rats; Fig. 1e); 50% of cells were located more than 600 μm (~6 or 7 glomeruli) from the injection site, and 10% more than 1,000 μm away (~10–12 glomeruli). When corrected for bulb size (glomerular layer surface area), there were no significant differences in cell distribution between rat and mouse.
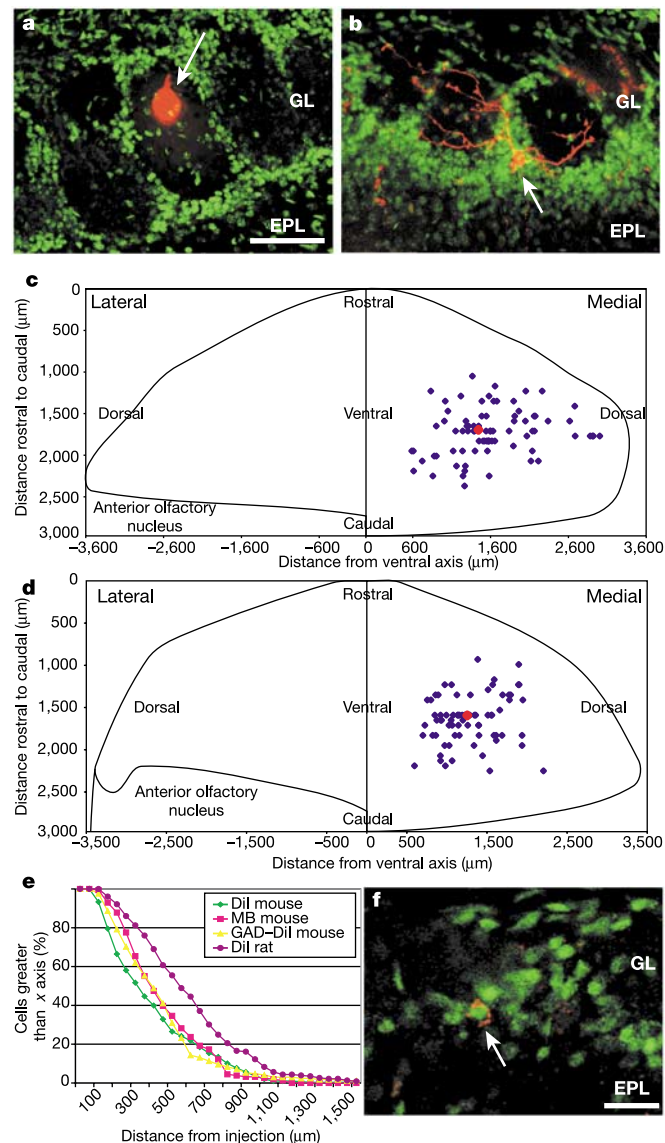
As DiI is taken up by all membranes and undergoes both anterograde and retrograde transport, rhodamine microbeads—a retrograde tracer taken up preferentially at synaptic endings[20]—were injected into the glomerular layer *in vivo* to confirm our anatomical results. The distribution of microbead-labelled cells from a single injection in each animal was similar to that seen with DiI (44.5 ± 13.7 cells, $n = 4$ mice; Fig. 1e, f), suggesting a widespread axonal, rather than dendritic, projection from these cells.

To investigate the trajectories of interglomerular axons, we used a novel *in vitro* parasagittal surface slice of the medial wall of the MOB (Fig. 2a). This 'surface slice' contained the olfactory nerve layer (ONL), the glomerular layer and the superficial external plexiform layer (EPL), but not the mitral cell layer and granule cell layer. This surface slice provided an 'aerial view' of most medial glomeruli. A single subglomerular-sized (5–10 μm diameter, $n = 16$ slices) iontophoretic DiI injection into each slice labelled a dense plexus of interglomerular connections (Fig. 2b). Interglomerular axons radiated in all directions with the highest process density within 500–600 μm of the injection site (Fig. 2b). Some processes were labelled as far as 2 mm from the injection site. This dense interglomerular network arose from only a small number of JG cells (59.5 ± 12.3 cells per slice), indicating that the cell type(s) interconnecting glomeruli have numerous axons and/or extensive axonal branching.
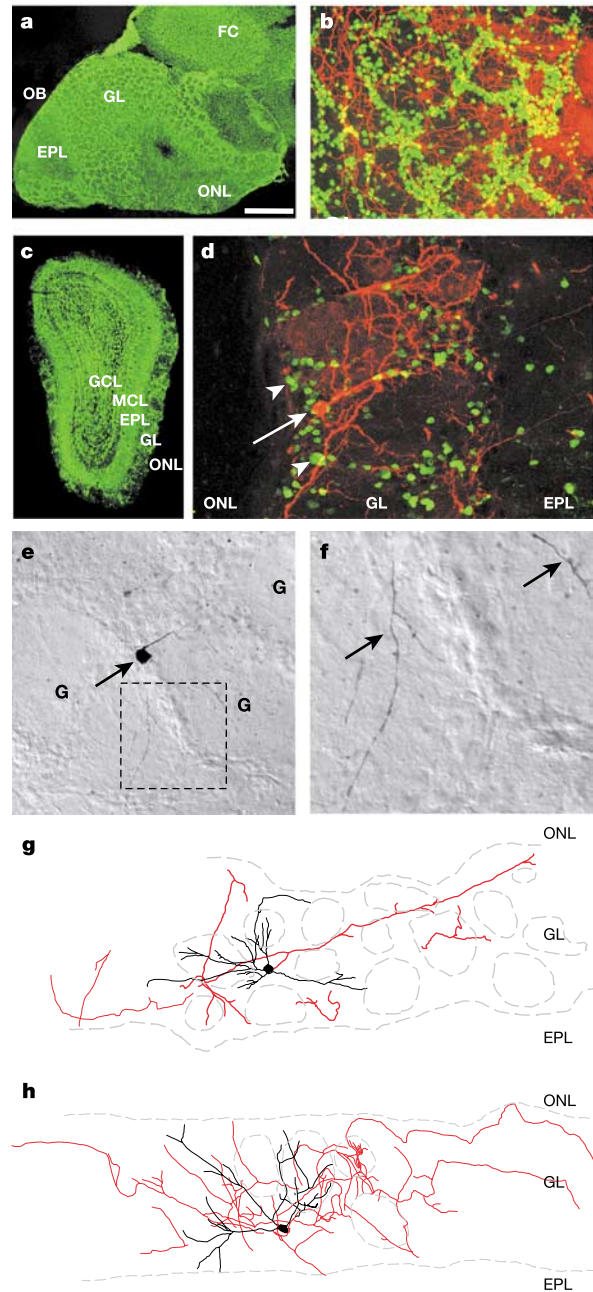
SA cells form interglomerular connections

Taken together, the tract-tracing results show that connections between olfactory bulb glomeruli are more substantial and extend

over far greater distances than was previously appreciated, but do not indicate which JG cell type(s) gives rise to this network. There are three principal types of JG neuron: periglomerular (PG), external tufted (ET) and short axon (SA) cells[17,18,19]. It has generally been thought that interglomerular connections are inhibitory and derive from GABA (γ-aminobutyric acid)-synthesizing PG cells[16], but there is little direct evidence for this. To investigate the role of GABAergic neurons in interglomerular projections, we made DiI injections in transgenic mice in which the promoter for glutamic acid decarboxylase 65 (GAD65, the principal GABA-synthesizing enzyme in the MOB[21]) drives the expression of green fluorescent protein (GFP; Fig. 2c). DiI injections into the glomerular layer of these mice (51 ± 15.8 cells per bulb, $n = 3$ mice; Fig. 1e) labelled
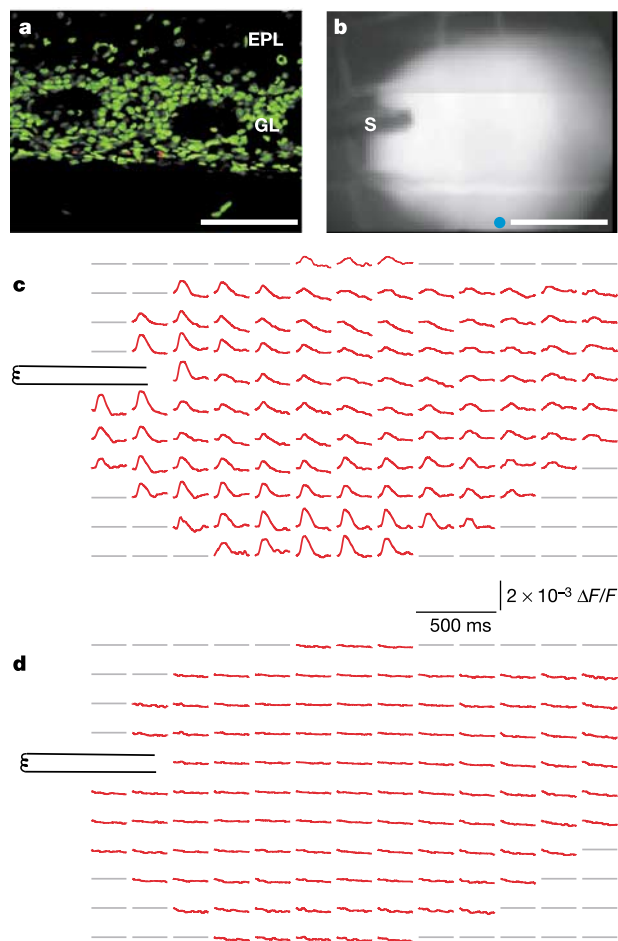
cells with a distribution identical to that of wild-type mice. However, only 9.1 ± 1.8% of DiI-labelled cells located one glomerulus or more from the injected glomerulus contained GFP (Fig. 2d and Supplementary Fig. 2). Therefore, the contribution of

Figure 2 Interglomerular connections derive from non-GABAergic 'short axon' cells. **a**, Surface slice showing the medial glomeruli stained with a nuclear counterstain (green). Owing to curvature of the bulb, areas of ONL, glomerular layer and EPL are visible in the same section. FC, frontal cortex; OB, olfactory bulb. **b**, DiI-labelled interglomerular connections form a dense plexus (injection off panel to right). **c**, Robust green fluorescence in GABAergic neurons in GAD65–GFP mice. GCL, granule cell layer; MCL, mitral cell layer. **d**, A subpopulation of PG cells expresses GFP (arrowheads). More than 90% of interglomerular projection cells lacked GFP (the arrow shows a DiI+ GFP− cell 350 μm from the injection site). **e**, Biocytin-filled SA cell soma situated between two glomeruli under DIC (differential interference contrast) optics. G, glomerulus. **f**, Demarcated region in **e** showing the thin SA cell axon extending through two glomeruli (arrows). **g**, **h**, Reconstruction of two biocytin-filled SA cells (dendrites, black; axon, red). Scale bar in **a** represents 1 mm in **a**; 100 μm in **b**; 500 μm in **c**; 25 μm in **d**, **e**; 10 μm in **f**; and 80 μm in **g**, **h**.

Figure 1 Extensive interglomerular connections shown by DiI and microbead tracing. **a**, Subglomerular-sized iontophoretic DiI injection into a single glomerulus (arrow). GL, glomerular layer. **b**, DiI-labelled JG cell bodies (arrowhead) within the glomerular layer (nuclei counterstained green). **c**, **d**, 'Flat plane' representations of the olfactory bulb glomerular layer from two experiments, showing the distribution of all labelled JG cells (cell bodies, blue dots; injection site, red dot). **e**, Percentage of labelled cells plotted as a function of distance from the injection site. Distributions in the larger rat bulb are significantly greater than those in the mouse ($P < 0.001$). MB, rhodamine microbeads. **f**, Microbead-labelled JG cells (arrows). Scale bar in **a** represents 50 μm and applies to **a** and **b**; scale bar in **f** represents 20 μm.

GABAergic cells to interglomerular connections is minor. Further-more, none of the labelled cells had prominent dendritic tufts characteristic of DiI-labelled ET cells, suggesting that ET cells do not contribute substantially to the interglomerular network.

We next analysed a population of over 200 physiologically characterized, biocytin-filled JG neurons available from other experiments. Neither PG nor ET cells had interglomerular axons projecting over the distances revealed by our tracing experiments. Only one cell type consistently had long axons within the glome-rular layer. This neuron had relatively thin axons (<0.5 μm diam-eter, $n = 11$ cells; Fig. 2e, f). These axons ramified up to 850 μm exclusively within the glomerular layer, with no obvious directional bias (Fig. 2g, h; total axon length, $3,625 \pm 816$ μm). The cells had 3–5 (3.2 ± 0.3) poorly branched dendrites that contacted 2–4 glomeruli (total dendrite length, $1,308 \pm 64$ μm). With the notable exception of the length and richness of their axonal trajectories, the morphological features of these cells correspond to the 'short axon' cell described in classical Golgi studies. Classical SA cells were said to have 3–5 'stout', infrequently branching dendrites that traverse 2–4 glomeruli, and a thin varicose axon projecting over 1–2 glome-ruli[17,22]. The greater extent of the axonal arborizations in biocytin-filled SA cells versus the 'short axons' seen in classical studies is
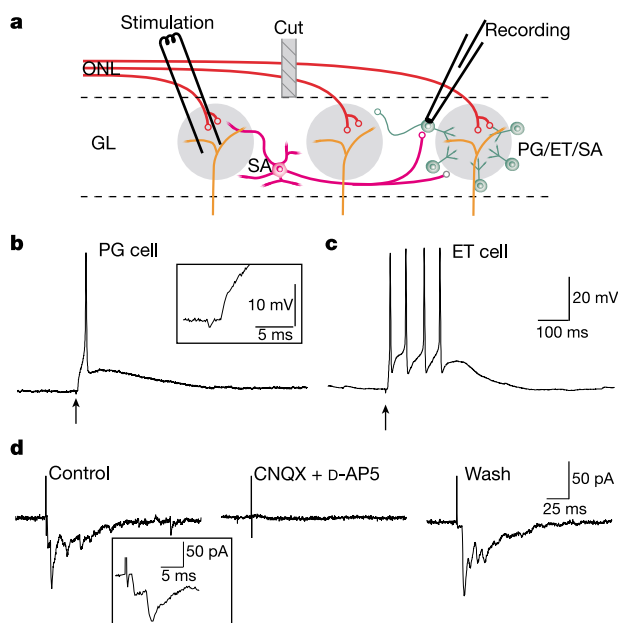
probably due to limited impregnation of axons achieved with the Golgi–Cox method[17,22]. Accordingly, we conclude that the main source of interglomerular connections is the SA cell.

Interglomerular connections are excitatory

Our anatomical findings demonstrate an extensive interglomerular network but provide no insight into its functional significance. To investigate the physiology of this system, we first used functional imaging. As the anatomical results indicate that interglomerular connections are not GABAergic, we reasoned that interglomerular connections might be glutamatergic. If true, then focal glomerular layer stimulation should, through the interglomerular network, cause widespread excitation of JG cells. To test this hypothesis, we used a voltage-sensitive dye to monitor changes in membrane potential after focal stimulation of the glomerular layer in a surface slice (Fig. 3). To prevent activation of olfactory nerve axons, the slices were taken from mice in which the olfactory nerve had been irreversibly ablated by $ZnSO_4$ lavage[23] of the olfactory mucosa 8–12 days before recording (Fig. 3a).

Focal glomerular stimulation ($n = 6$ slices) evoked widespread depolarization throughout the glomerular layer (Fig. 3c). The depolarizing response spread in all directions from the stimulating electrode, extending 900 ± 93 μm along the long axis of the MOB (rise time, 51.3 ± 4.7 ms; half-width, 51.4 ± 8.3 ms). These wide-spread depolarizing responses were abolished by the addition of the ionotropic glutamate receptor antagonists APV (D-2-amino-5-phosphonopentanoate; 50 μM) and CNQX (6-cyano-7-nitro-quinoxaline-2,3-dione; 10 μM) ($n = 3$; Fig. 3d). Responses recovered after 40 min of washout. These results show that interglomerular connections are extensive, excitatory and mediated by glutamate acting at ionotropic receptors.

Although the VSD (voltage-sensitive dye) imaging results indi-cate that excitatory synapses underlie a substantial proportion of interglomerular connections, they do not exclude some contri-bution of long-range inhibitory connections. To further investigate
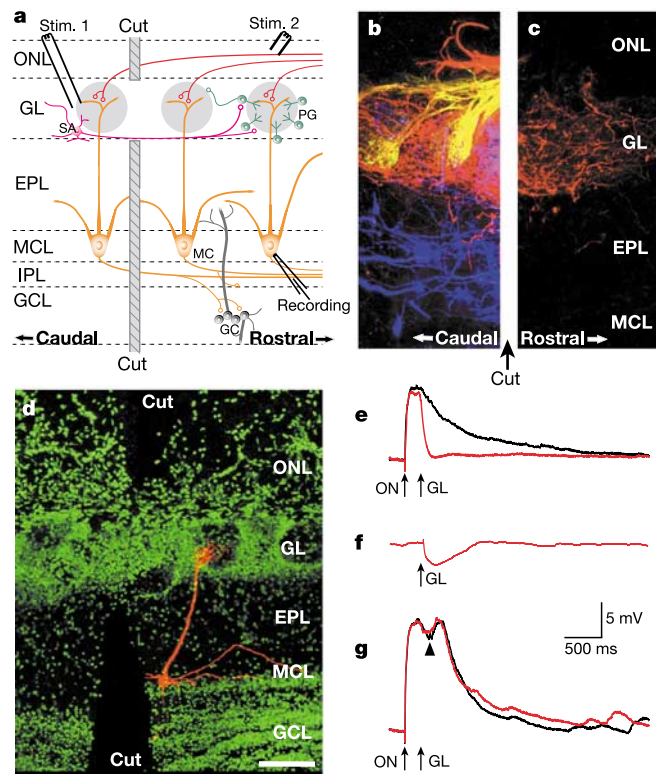
Figure 3 Functional imaging shows extensive interglomerular excitation. **a**, DiD tracing confirming the elimination of olfactory nerve axons (red) in the glomerular layer of a mouse after ablation by $ZnSO_4$ lavage. **b**, Fluorescence image of a parasagittal surface slice loaded *in vitro* with the voltage-sensitive dye RH414. The cyan circle shows the approximate diameter of a single mouse glomerulus. s, stimulating electrode. **c**, Spatial averages (100 × 100 μm) of optical signals evoked by glomerular stimulation. Stimulation induces widespread depolarization (upward deflection in the inverted traces). **d**, Responses were abolished when glutamatergic transmission was blocked. Scale bars represent 100 μm in **a** and 500 μm in **b**.

Figure 4 Interglomerular connections excite juxtaglomerular cells. **a**, Schematic of the experimental design. **b**, **c**, PG cells (**b**) and ET cells (**c**) responded with EPSPs to distant glomerular layer stimulation (arrow). The inset (expanded) shows a 2 ms response latency, consistent with a monosynaptic event. **d**, Voltage-clamp recordings of an EPSC in a PG cell following distant glomerular layer stimulation (left). The inset (expanded) shows 1.8 ms EPSC response latency. The EPSC was abolished when glutamatergic transmission was blocked (middle), and recovered after washout (right).

the circuit actions of interglomerular connections, whole-cell recordings were made from JG cells 3 or 4 glomeruli away from the site of focal glomerular stimulation in MOB slices. The ONL was severed between the stimulation and recording sites to prevent propagation through olfactory nerve fibres (Fig. 4a). Fourteen biocytin-filled JG cells that responded to glomerular layer stimulation were classified according to established morphological criteria[19,22,24]: 10 (72%) were PG cells, 3 (21%) were ET cells, and 1 (7%) was an SA cell. Most of these cells (93%, 13 of 14) responded with excitatory postsynaptic potentials (EPSPs) after distant glomerular layer stimulation (Fig. 4b, c), whereas only one PG cell responded with an inhibitory postsynaptic potential (IPSP). Response latencies were 2.1 ± 0.2 ms for EPSPs, and 1.8 ms for the single case of an IPSP, consistent with monosynaptic events. Evoked EPSPs were abolished in the presence of ionotropic glutamate receptor antagonists (APV and CNQX; $n = 6$; Fig. 4d). These results further support the conclusion that most interglomerular connections are excitatory and glutamatergic.
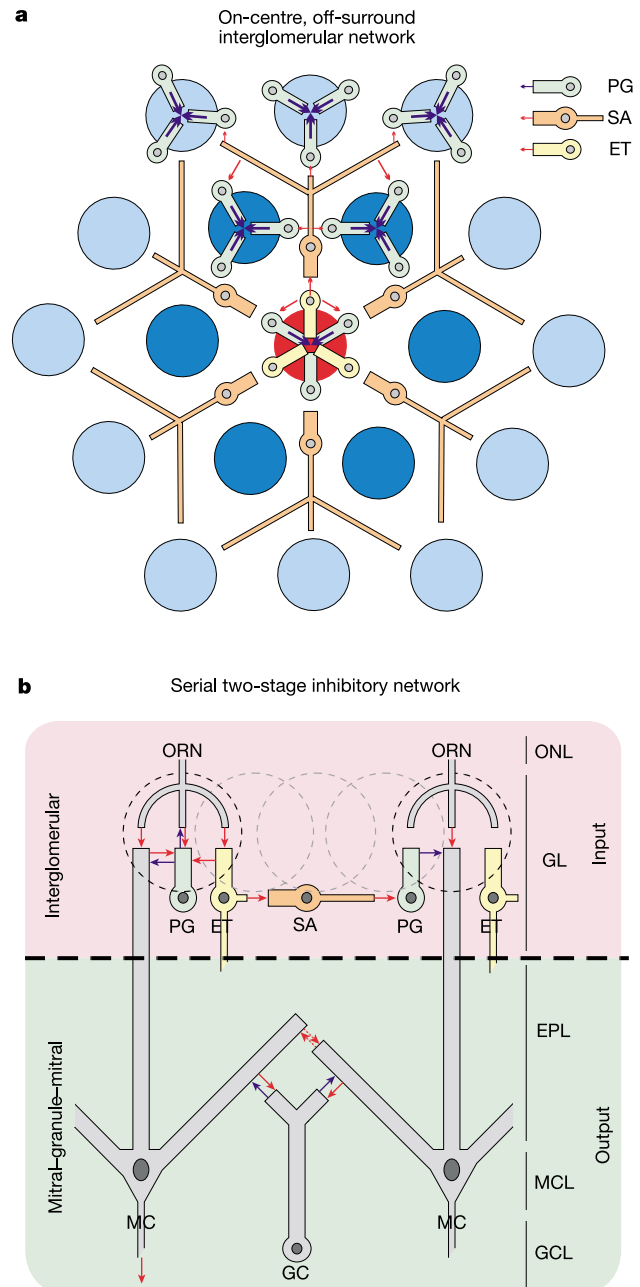
Centre–surround inhibition among glomeruli

Taken together, these results show that SA cells form an extensive network of excitatory interglomerular connections that release glutamate and excite PG cells. PG cells are thought to form GABAergic[25] inhibitory synapses with the dendrites of mitral cells. Therefore, activation of interglomerular connections should inhibit mitral cell responses to olfactory nerve input. To test this hypothesis, we recorded mitral cell responses to olfactory nerve stimulation in MOB slices[26] that had been surgically altered to allow interglomerular connections to be stimulated in isolation. Microsurgical cuts were made through the ONL and all deep layers, leaving only the

Figure 5 Interglomerular connections inhibit mitral cell responses to olfactory nerve input. **a**, Schematic of the experimental design. **b**, Microinjections of DiA, DiI and DiD into the ONL, glomerular layer and EPL, respectively, caudal to the cuts label processes coursing tangentially through intact regions of the slice. GC, granule cell; IPL, internal plexiform layer; MC, mitral cell. **c**, On the opposite side of the cuts (rostral), only interglomerular connections are intact. **d**, Biocytin-filled mitral cell (red) and nuclear counterstain (green). The cuts through the ONL and deep bulb layers are clearly visible. **e**, Mitral cells respond to ONL stimulation with an LLD (black trace) that is abruptly terminated by distant glomerular layer stimulation (arrow, red trace). ON, olfactory nerve. **f**, Stimulation of interglomerular connections evokes an IPSP in mitral cells. **g**, In the presence of gabazine, olfactory-nerve-evoked LLDs are no longer suppressed by glomerular layer stimulation (black trace, olfactory nerve stimulation alone; red trace, olfactory nerve plus interglomerular stimulation). Consistent with blockade of inhibition, the LLD is larger and has an additional peak (arrowhead). The scale bar in **d** represents 100 μm in **b**–**d**.

Figure 6 Centre–surround inhibitory networks in the olfactory bulb. **a**, Schematic of the on-centre, off-surround inhibitory network in the glomerular layer (red arrows, excitatory connections; blue arrows, inhibitory). An activated glomerulus (red) causes widespread inhibition (blue) of surrounding glomeruli by the interglomerular network. **b**, Schematic showing two serial levels of MOB centre–surround inhibition: interglomerular and mitral–granule–mitral. The interglomerular circuit at the level of olfactory nerve input is formed by SA cells that excite PG and ET cells in distant glomeruli. Activation of GABAergic PG cells causes inhibition of mitral cells. The mitral–granule–mitral network at the level of mitral cell output is formed by mitral cells exciting granule cells, which in turn inhibit the same (feedback) and other (feedforward) mitral cells.

glomerular layer intact between opposite sides of the cuts (Fig. 5a–d). The olfactory nerve was stimulated and mitral cell responses recorded on one side of the cuts while interglomerular connections were stimulated on the other side. After recording, we made microinjections of DiA, DiI and DiD into the ONL, glomerular layer and EPL, respectively. This tracing showed that only interglomerular connections were intact (Fig. 5b, c). Biocytin fills of recorded mitral cells showed that processes on the side of the cut were severed (Fig. 5d) and that the apical dendrite was intact.

Mitral cells respond to olfactory nerve stimulation with a long-lasting depolarization (LLD)[27]. Activation of interglomerular connections excites GABAergic PG cells and should, therefore, inhibit evoked LLDs in mitral cells. Indeed, stimulation of interglomerular connections abruptly terminated olfactory-nerve-evoked LLDs in 6 of 7 mitral cells recorded 150–525 μm distal to glomerular layer stimulation (Fig. 5e). Glomerular stimulation reduced LLD magnitude, calculated by integrated voltage under the curve, to 0.15% of control ($n = 6$, $P < 0.01$). Thus, input from distant regions of the glomerular layer inhibits mitral cell responses to olfactory nerve input. Mean latency from olfactory nerve stimulation to LLD onset—a monosynaptic event—was 2.9 ± 0.2 ms, and mean latency from interglomerular stimulation to the onset of LLD termination was 6.5 ± 1.2 ms. This latency suggests that interglomerular connections inhibit mitral cells through monosynaptic activation of GABAergic PG cells or disynaptic activation of ET cells that monosynaptically excite PG cells, or both.

Interglomerular excitation of PG cells should thus generate a summated IPSP in glomerular tufts of mitral cells sufficient to terminate the LLD. Detection of IPSPs in mitral cell glomerular tufts is limited by remoteness from the somatic recording site. To enhance detection of distal IPSPs, mitral cells were held 30 mV positive to the Cl⁻ equilibrium potential (at −55 to −50 mV, $E_{Cl} = -84$ mV). In 3 of 4 mitral cells in which LLDs were terminated by interglomerular stimulation, an IPSP was detectable (mean response latency, 5.7 ± 0.9 ms, $n = 3$; Fig. 5f). As other potential sources of inhibitory input were excluded by microsurgical cuts, these IPSPs must be generated in the apical tuft of the mitral cell by interglomerular activation of GABAergic PG cells.

If interglomerular connections act through PG cells to attenuate the LLD, this action should be abolished by blockade of GABAergic transmission. Application of the GABA_A receptor blocker gabazine (5 μM) increased LLD magnitude and introduced additional peaks in the response (Fig. 5g), consistent with the suppression of tonic GABAergic inhibition. Importantly, in the presence of gabazine, stimulation of interglomerular connections no longer attenuated olfactory-nerve-evoked LLDs (Fig. 5g). The effect of gabazine reversed after 40 min of washout. These experiments show that excitatory interglomerular connections activate local GABAergic PG cells to cause postsynaptic inhibition of mitral cell responses to olfactory nerve input.

Discussion

Centre–surround inhibition is a fundamental mechanism in sensory processing[28] that enhances contrast between populations of strongly and weakly excited neurons. The best-characterized inhibitory circuit in the MOB involves lateral inhibition of mitral cells at mitral–granule cell synapses in the EPL[16,29,30]. By comparison, virtually nothing is known about centre–surround inhibition in the glomerular layer, the initial site of synaptic processing in the olfactory system. The findings presented here demonstrate the presence of long-range interconnections between glomeruli, extending up to 2 mm (20–30 glomeruli radii). These connections excite PG cells in distant glomeruli, causing inhibition of mitral cell responses to olfactory nerve input. This interglomerular network provides on-centre, off-surround processing at the initial stage of synaptic integration in the MOB (Fig. 6a). By enhancing spatial contrast between patterns of odour-evoked glomerular activity at

the level of sensory input, centre–surround processing may be a key first step in the neural computation of odours.

Our findings show that SA cells are the principal JG neuron type making interglomerular connections. The classical picture of interglomerular connections was based on the Golgi–Cox staining studies of Cajal and Golgi[22,24], and the EM, Golgi and degeneration studies of Pinching and Powell[17–19,31]. The axonal projections of SA cells were reported to extend only 1–3 glomeruli from the cell soma[19,22]. However, as the Golgi–Cox method stains axons incompletely[17,22], the classical view of the SA cell underestimated the extent of its axonal arborization. Indeed, our DiI and microbead tracer experiments, and reconstructions of individual biocytin-filled neurons, showed that SA cell axons extend several millimetres within the glomerular layer.

Imaging studies of olfactory nerve terminals loaded with calcium-sensitive dyes, which reflect only presynaptic olfactory nerve terminal activity, show that individual or small groups of glomeruli are activated by low concentrations of single odorants[32,33]. By contrast, studies with 2-deoxyglucose (2-DG)[9,34–36], c-fos[37,38] and functional magnetic resonance imaging (fMRI)[13], which reflect the activation of pre- and/or postsynaptic elements, show broader regions of activity spanning multiple glomeruli. The interglomerular connections reported here may reconcile these disparate observations. As activation of a single glomerulus excites JG cells hundreds of micrometres away, methods such as 2-DG, c-fos and fMRI may reflect initial activation of a few discrete glomeruli by a single odorant followed by synaptic activation of JG cells in multiple neighbouring glomeruli through the interglomerular circuit.

Interglomerular connections synapse not only onto PG cells but also onto ET cells and other SA cells. ET cells excite PG and SA cells associated with the same glomerulus. Martinez and Freeman observed an excitatory field potential at the glomerular layer–EPL border, thought to reflect activity in mitral[39] and/or tufted cells. Interglomerular excitation of SA and ET cells may underlie these excitatory field potentials. In the intact bulb, sequential excitation of ET and SA cells could propagate activity over very long distances in the glomerular layer.

On-centre, off-surround organization in the MOB has generally been attributed to synaptic interactions between the lateral dendrites of mitral cells and inhibitory granule cells in the EPL[15,16]. In this mitral–granule–mitral circuit, strongly-activated mitral cells[40] laterally inhibit weakly-activated surrounding mitral cells. The interglomerular circuit reported here also forms a centre–surround organization: activation of a glomerulus—'on-centre'—should cause widespread inhibition of mitral cells in neighbouring glomeruli—'off-surround'. Thus, the current findings add a new dimension to our understanding of the functional organization of the olfactory bulb by showing that there are two serial stages of centre–surround inhibition (Fig. 6b). Neural network modelling suggests that two serial stages of centre–surround inhibition are highly advantageous to sensory networks[41,42]. The first stage is the interglomerular circuit, which operates at the level of olfactory nerve sensory input. It is formed by SA cells that make excitatory interglomerular connections onto inhibitory PG cells, which in turn inhibit mitral cells. This stage also provides presynaptic regulation of transmitter release from olfactory nerve terminals[32,43]. This stage may preserve relative response magnitudes across a range of input intensities (pattern normalization), reduce noise (low-band filtration) and enhance contrast between activated glomeruli. The second stage operates at the level of mitral cell output. It is formed by the mitral–granule–mitral circuit. The second stage may prevent response saturation at high input intensities and provide further contrast enhancement[42]. Together, these two centre–surround circuits may synergistically enhance patterns of olfactory input.

The neural representation of odour refined by these two stages of inhibition need not be static, and probably involves spatiotemporal changes in the distribution of activity in the MOB[44]. In this view, the

mitral–granule–mitral circuit serves to progressively sharpen odour representations in the neuronal population, rather than simply sharpening the tuning curves of individual mitral cells. However, because the mitral–granule–mitral circuit will amplify differences in patterns of glomerular activity[44], pattern normalization and effective noise reduction is needed at the first stage of input to the olfactory bulb, operations that may be performed by the centre–surround interglomerular network. □

Methods

Tracer injections

For whole-brain staining with DiI, adult (5-week-old) mice (CD-1 and transgenic GAD65–GFP; the generation of these mice will be published elsewhere) and rats (Sprague–Dawley) were anaesthetized (150 mg kg^{-1} Nembutal) and transcardially perfused with 4% paraformaldehyde in 0.1 M phosphate buffer (PFA; pH 7.4). Their brains were removed and a single glomerulus in each MOB injected iontophoretically with DiI (1 mg ml^{-1} in ethanol, 0.5–2.0 μA, tip diameter 1.5 μm). Brains were incubated at 23 °C in PFA for 2 weeks, serially sectioned (60 μm in the coronal plane), incubated in 20 nM Sytox Green (Molecular Probes) in PBS for 30 min (CD1 and rat) and coverslipped with a DABCO-based mounting media.

For the DiI staining of parasagittal surface slices, brains from adult mice were removed, hemisected and positioned in low-gel agarose with the medial surface parallel to the plane of the vibratome. A single 350 μm section was cut from the medial surface of each MOB and immobilized in a recording chamber perfused with artificial cerebral spinal fluid (ACSF) containing 120 mM NaCl, 8 mM KCl, 1.3 mM CaCl$_2$, 1.3 mM MgSO$_4$, 10 mM glucose, 25 mM NaHCO$_3$ and 5 mM BES, and saturated with 95% O$_2$/5% CO$_2$. This 'surface slice' contained the entire medial wall ONL, glomerular layer and part of the EPL. A single glomerulus was iontophoretically injected with DiI, incubated at 23 °C in PFA for 2 weeks, resectioned (50 μm in the sagittal plane) and stained with Sytox.

For whole-brain staining with microbeads, adult CD-1 mice were anaesthetized and 10–20 nl of rhodamine-labelled latex microbeads (Lumafluor; 1:2 dilution in saline) were injected into the medial glomerular layer of the left MOB (stereotaxic coordinates 4.28 mm Bregma, 1.02 mm depth, 0.12 mm lateral). The injection pipette was positioned 4.8 mm lateral at 55° over the right MOB, and inserted through the right MOB into the left MOB glomerular layer (1.25 mm from the right MOB surface). After one week, mice were transcardially perfused, and the brain was serially sectioned (40 μm in the coronal plane) and stained with Sytox.

Sections were visualized at high magnification and the position of labelled JG cell somata plotted on a camera lucida outline. The rostrocaudal distance (z axis) of each cell was measured from the section number, and the dorsoventral (x axis) and mediolateral (y axis) coordinates automatically measured using the Image Processing Toolkit (Reindeer Graphics). These coordinates were used to generate reverse cumulative probability graphs of cell distance from the injection using a custom Excel worksheet. Statistical significance was tested by analysis of variance (ANOVA; Scheffe's post hoc test; all values presented as mean ± s.e.m.). The surface of each MOB was presented as an unfolded sheet—a 'flat plane' representation—by tracing the glomerular layer in each section and 'unfolding' these traces into a flattened sheet.

SA cell reconstructions

SA cells were recorded in horizontal rat MOB slices (400 μm) as previously described[26]. The pipette filling solution contained 0.5% biocytin, 125 mM potassium gluconate, 2 mM MgCl$_2$, 10 mM HEPES, 2 mM Mg$_2$ATP, 0.2 mM Na$_3$GTP, 1 mM NaCl and 0.2 mM EGTA, pH 7.2. After recording, slices were fixed in PFA, resectioned (80 μm) and reacted with ABC reagent (Vector Laboratories) and diaminobenzidine following standard protocols. Cells were reconstructed using Neurolucida (Microbrightfield).

Optical recordings

Membrane potential changes were visualized using the voltage-sensitive dye RH414 (Molecular Probes)[45,46]. Surface slices were prepared from 5–6-week-old mice. The olfactory nerve had been irreversibly destroyed by lavage of the epithelium with ZnSO$_4$ (ref. 23) 8–12 days before slicing. To confirm the extent of this lesion, several mice were transcardially perfused and the nasal cavities flushed with 5 mg ml^{-1} DiD in ethanol, incubated at 30 °C for 2 weeks, sectioned and imaged.

Surface slices were incubated in constant-flow ACSF for 30 min at 30 °C, then 200 μM RH414 in ACSF for 30 min at 23 °C, and transferred to a recording bath at 23 °C. Images were captured at 2 kHz through a ×10 water immersion objective with a NeuroCCD camera and analysed in NeuroPlex (RedShirtImaging). Slices were illuminated with a stabilized 150 W Xenon lamp (Opti-Quip) with exposure regulated by electronic shutter (Uniblitz, Vincent Associates). Constant-current stimuli (100–300 μA) were applied through a bipolar stimulating electrode.

Electrophysiology

JG cells were recorded in horizontal rat MOB slices with the glomerular layer stimulated (100–300 μA) 3–4 glomeruli from the recording site; the ONL between stimulation and recording sites was transected perpendicular to the glomerular layer.

To record from mitral cells, horizontal mouse MOB slices (350 μM) were prepared with opposing cuts made perpendicular to the glomerular layer through the ONL and all deep layers (EPL to granule cell layer), leaving only the glomerular layer intact. Mitral cells on the rostral side of the cuts were recorded in whole-cell current clamp (held at −70 mV to prevent action potentials). The ONL was stimulated rostral to the cuts and

interglomerular connections stimulated with a second electrode positioned in the glomerular layer caudal to the cuts. The olfactory nerve was stimulated with and without subsequent stimulation (200 ms delay) of the distant glomerular layer. This interval allowed the interglomerular circuit to be investigated without involvement of olfactory-nerve-evoked presynaptic effects[47]. Olfactory nerve stimulation intensity was the minimum sufficient to activate a LLD in 100% of trials (80–300 μA, 0.1 ms, 0.2 Hz). Glomerular layer stimulation intensity was 300–500 μA. Sets of at least 20 stimuli in each condition were averaged and area under the voltage traces measured. Statistical significance was tested using Student's paired two-sample t-test (all values presented as mean ± s.e.m.). After recording, biocytin was visualized with streptavidin-Cy3 (Jackson) or the completeness of cuts verified with lipophilic tract tracing. DiA, DiI and DiD were injected into the ONL, glomerular layer and EPL, respectively, and incubated at 30 °C for one week.

1. Ressler, K. J., Sullivan, S. L. & Buck, L. B. A zonal organization of odorant receptor gene expression in the olfactory epithelium. Cell 73, 597–609 (1993).
2. Mombaerts, P. et al. The molecular biology of olfactory perception. Cold Spring Harb. Symp. Quant. Biol. 61, 135–145 (1996).
3. Vassar, R. et al. Topographic organization of sensory projections to the olfactory bulb. Cell 79, 981–991 (1994).
4. Potter, S. M. et al. Structure and emergence of specific olfactory glomeruli in the mouse. J. Neurosci. 21, 9713–9723 (2001).
5. Treloar, H. B., Feinstein, P., Mombaerts, P. & Greer, C. A. Specificity of glomerular targeting by olfactory sensory axons. J. Neurosci. 22, 2469–2477 (2002).
6. Greer, C. A., Stewart, W. B., Kauer, J. S. & Shepherd, G. M. Topographical and laminar localization of 2-deoxyglucose uptake in rat olfactory bulb induced by electrical stimulation of olfactory nerves. Brain Res. 217, 279–293 (1981).
7. Halasz, N. & Greer, C. A. Terminal arborizations of olfactory nerve fibers in the glomeruli of the olfactory bulb. J. Comp. Neurol. 337, 307–316 (1993).
8. Jastreboff, P. J. et al. Specific olfactory receptor populations projecting to identified glomeruli in the rat olfactory bulb. Proc. Natl Acad. Sci. USA 81, 5250–5254 (1984).
9. Johnson, B. A. & Leon, M. Modular representations of odorants in the glomerular layer of the rat olfactory bulb and the effects of stimulus concentration. J. Comp. Neurol. 422, 496–509 (2000).
10. Johnson, B. A. & Leon, M. Spatial distribution of [^{14}C]2-deoxyglucose uptake in the glomerular layer of the rat olfactory bulb following early odor preference learning. J. Comp. Neurol. 376, 557–566 (1996).
11. Rubin, B. D. & Katz, L. C. Optical imaging of odorant representations in the mammalian olfactory bulb. Neuron 23, 499–511 (1999).
12. Xu, F., Kida, I., Hyder, F. & Shulman, R. G. Assessment and discrimination of odor stimuli in rat olfactory bulb by dynamic functional MRI. Proc. Natl Acad. Sci. USA 97, 10601–10606 (2000).
13. Yang, X. et al. Dynamic mapping at the laminar level of odor-elicited responses in rat olfactory bulb by functional MRI. Proc. Natl Acad. Sci. USA 95, 7715–7720 (1998).
14. Rubin, B. D. & Katz, L. C. Spatial coding of enantiomers in the rat olfactory bulb. Nature Neurosci. 4, 355–356 (2001).
15. Mori, K., Nagao, H. & Yoshihara, Y. The olfactory bulb: coding and processing of odor molecule information. Science 286, 711–715 (1999).
16. Yokoi, M., Mori, K. & Nakanishi, S. Refinement of odor molecule tuning by dendrodendritic synaptic inhibition in the olfactory bulb. Proc. Natl Acad. Sci. USA 92, 3371–3375 (1995).
17. Pinching, A. J. & Powell, T. P. Experimental studies on the axons intrinsic to the glomerular layer of the olfactory bulb. J. Cell Sci. 10, 637–655 (1972).
18. Pinching, A. J. & Powell, T. P. The neuropil of the periglomerular region of the olfactory bulb. J. Cell Sci. 9, 379–409 (1971).
19. Pinching, A. J. & Powell, T. P. The neuron types of the glomerular layer of the olfactory bulb. J. Cell Sci. 9, 305–345 (1971).
20. Cornwall, J. & Phillipson, O. T. Quantitative analysis of axonal branching using the retrograde transport of fluorescent latex microspheres. J. Neurosci. Methods 24, 1–9 (1988).
21. Sheikh, S. N., Martin, S. B. & Martin, D. L. Regional distribution and relative amounts of glutamate decarboxylase isoforms in rat and mouse brain. Neurochem. Int. 35, 73–80 (1999).
22. Cajal, R. S. Histologie du Systeme Nerveux de l'Homme et des Vertebres (Maloine, Paris, 1911).
23. Kawano, T. & Margolis, F. L. Transsynaptic regulation of olfactory bulb catecholamines in mice and rats. J. Neurochem. 39, 342–348 (1982).
24. Golgi, C. Sulla Fina Struttura dei Bulbi Olfattorii (Reggio-Emilia, Rome, 1875).
25. Mugnaini, E., Oertel, W. H. & Wouterlood, F. F. Immunocytochemical localization of GABA neurons and dopamine neurons in the rat main and accessory olfactory bulbs. Neurosci. Lett. 47, 221–226 (1984).
26. Heyward, P., Ennis, M., Keller, A. & Shipley, M. T. Membrane bistability in olfactory bulb mitral cells. J. Neurosci. 21, 5311–5320 (2001).
27. Carlson, G. C., Shipley, M. T. & Keller, A. Long-lasting depolarizations in mitral cells of the rat olfactory bulb. J. Neurosci. 20, 2011–2021 (2000).
28. Shepherd, G. M. The Synaptic Organization of the Brain (Oxford Univ. Press, New York, 1990).
29. Chen, W. R., Shen, G. Y., Shepherd, G. M., Hines, M. L. & Midtgaard, J. Multiple modes of action potential initiation and propagation in mitral cell primary dendrite. J. Neurophysiol. 88, 2755–2764 (2002).
30. Chen, W. R., Xiong, W. & Shepherd, G. M. Analysis of relations between NMDA receptors and GABA release at olfactory bulb reciprocal synapses. Neuron 25, 625–633 (2000).
31. Pinching, A. J. & Powell, T. P. The neuropil of the glomeruli of the olfactory bulb. J. Cell Sci. 9, 347–377 (1971).
32. Wachowiak, M. & Cohen, L. B. Presynaptic inhibition of primary olfactory afferents mediated by different mechanisms in lobster and turtle. J. Neurosci. 19, 8808–8817 (1999).
33. Wachowiak, M. & Cohen, L. B. Presynaptic afferent inhibition of lobster olfactory receptor cells: reduced action-potential propagation into axon terminals. J. Neurophysiol. 80, 1011–1015 (1998).
34. Astic, L. & Cattarelli, M. Metabolic mapping of functional activity in the rat olfactory system after a bilateral transection of the lateral olfactory tract. Brain Res. 245, 17–25 (1982).

35. Benson, T. E., Burd, G. D., Greer, C. A., Landis, D. M. & Shepherd, G. M. High-resolution 2-deoxyglucose autoradiography in quick-frozen slabs of neonatal rat olfactory bulb. *Brain Res.* **339,** 67–78 (1985).

36. Johnson, B. A., Woo, C. C. & Leon, M. Spatial coding of odorant features in the glomerular layer of the rat olfactory bulb. *J. Comp. Neurol.* **393,** 457–471 (1998).

37. Guthrie, K. M. & Gall, C. M. Functional mapping of odor-activated neurons in the olfactory bulb. *Chem. Senses* **20,** 271–282 (1995).

38. Onoda, N. Odor-induced fos-like immunoreactivity in the rat olfactory bulb. *Neurosci. Lett.* **137,** 157–160 (1992).

39. Martinez, D. P. & Freeman, W. J. Periglomerular cell action on mitral cells in olfactory bulb shown by current source density analysis. *Brain Res.* **308,** 223–233 (1984).

40. Isaacson, J. S. Glutamate spillover mediates excitatory transmission in the rat olfactory bulb. *Neuron* **23,** 377–384 (1999).

41. Grossberg, S. Neural pattern discrimination. *J. Theor. Biol.* **27,** 291–337 (1970).

42. Grossberg, S. Adaptive pattern classification and universal recoding: I. Parallel development and coding of neural feature detectors. *Biol. Cybern.* **23,** 121–134 (1976).

43. Aroniadou-Anderjaska, V., Ennis, M. & Shipley, M. T. Glomerular synaptic responses to olfactory nerve input in rat olfactory bulb slices. *Neuroscience* **79,** 425–434 (1997).

44. Laurent, G. *et al.* Odor encoding as an active, dynamical process: experiments, computation, and theory. *Annu. Rev. Neurosci.* **24,** 263–297 (2001).

45. Kauer, J. S., Senseman, D. M. & Cohen, L. B. Odor-elicited activity monitored simultaneously from 124 regions of the salamander olfactory bulb using a voltage-sensitive dye. *Brain Res.* **418,** 255–261 (1987).

46. Kauer, J. S. Real-time imaging of evoked activity in local circuits of the salamander olfactory bulb. *Nature* **331,** 166–168 (1988).

47. Aroniadou-Anderjaska, V., Zhou, F. M., Priest, C. A., Ennis, M. & Shipley, M. T. Tonic and synaptically evoked presynaptic inhibition of sensory input to the rat olfactory bulb via GABA$_B$ heteroreceptors. *J. Neurophysiol.* **84,** 1194–1203 (2000).

Correspondence and requests for materials should be addressed to M.T.S. (mshipley@umaryland.edu).